  DOI 10.1515/HTMP.2011.058

# Production of Silicon-based Nano-scale Materials Through High Temperature Reduction of Silica by Titanium

**Osamu Terakado,**[1,*] **Takeshi Nagata,**[1]
**Yoshinori Fujimoto**[1] **and Masahiro Hirasawa**[1]

[1] Department of Materials Science and Engineering, Graduate School of Engineering, Nagoya University, Nagoya, Japan

**Abstract.** The reduction of silica by titanium at 2073 K has been studied in order to develop a production process of silicon-based nano-scale materials. The silicon monoxide vapour, reaction intermediate products, has been transferred by argon carrier gas to colder parts of the reactor, which results in the disproportionation reaction to form Si and $SiO_2$. The products include particles with diameter of 10–100 nm order and wires. An attempt to remove $SiO_2$ by hydrofluoric acid treatment of the reduction products resulted in the enrichment of Si particles.

**Keywords.** Silicon, nano-materials, high temperature reduction, silica, titanium.

**PACS®(2010).** 81.07.-b, 81.20.-n, 82.30.Lp.

## 1 Introduction

Silicon-based nano-materials are of great importance in various fields, such as microelectronics. Precise control of nano-scale structure exhibits high efficiency in light emission, attracting researchers to develop useful silicon-based optical devices [1]. In the view of the steady increase in the demand of the silicon-based nano-materials, great attention should be paid in their effective production process. One of the promising methods is to utilize the disproportionation reaction of silicon monoxide, represented by $2SiO \rightarrow Si + SiO_2$ [2–4].

In our previous papers, we reported the carbothermic reduction of silica-containing slag to produce variety of nano-sized Si-based materials [5, 6]. The process consists of the formation of SiO vapour by the carbothermic reduction of slag and the consequent transfer of SiO-containing vapour to cold part of the reactor, which leads to the deposition and then the disproportionation reaction. We found the reasonable correlation between the morphology of the products and the process parameters including deposition temperature and carrier gas flow rate. This smelting process can be relatively easily scaled-up for the production of nano-sized silicon-based materials in large amount. On the other hand, the contamination of silicon carbide, formed presumably by the following reactions, cannot be avoided in carbothermic reduction:

$$2C(s) + SiO(g,l) = SiC(s) + CO(g),$$
$$3SiO(g,l,s) + CO(g) = SiC(s) + 2SiO_2(s),$$
$$SiO(g,l,s) + 3CO(g) = SiC(s) + 2CO_2(g).$$

A chemical analysis showed that more than 10 atomic percents of carbon is included in the reaction products [6]. One possibility to overcome the difficulty is not to use carbon but other reducing agent, such as reactive metals, e.g., aluminium and titanium. In the present paper we address the results of reduction of $SiO_2$ by titanium at 2073 K. The characteristics of the reaction products are presented. Moreover, an attempt was made to increase the yield of silicon by treating the reaction products with aqueous hydrofluoric acid solution which removes silica according to the following reactions:

$$SiO_2 + 6HF(aq) = H_2SiF_6(l) + 2H_2O,$$
$$SiO_2 + 4HF(g) = SiF_4(g) + 2H_2O.$$

## 2 Experimental Procedure

### 2.1 Materials

Sample was prepared by mixing the powders of $SiO_2$ (Quartz, 99.9 %, Particle size = ca. 0.8 μm, Kojundo Chem. Lab.) and Ti (99.9 %, Particle size under 45 μm, Kojundo Chem. Lab.). The compositions of $[SiO_2] : [Ti] = 1 : 0.5$, $1 : 0.7$, $1 : 1$ and $1 : 2$ in molar ratio were examined. In a typical experimental run, total weight of mixture was 15 g for $[SiO_2] : [Ti] = 1 : 2$ and 12 g for other compositions. Prior to the high temperature reaction, a few millilitres of starch solution were added as a binder to the mixture, which was then pelletized to several discs with the diameter of 8 mm.

**Corresponding author:** Osamu Terakado, Department of Materials Science and Engineering, Graduate School of Engineering, Nagoya University, Furo-cho, Chikusa-ku, 464-8603 Nagoya, Japan;
E-mail: teramon@numse.nagoya-u.ac.jp.

Received: January 31, 2011. Accepted: April 15, 2011.

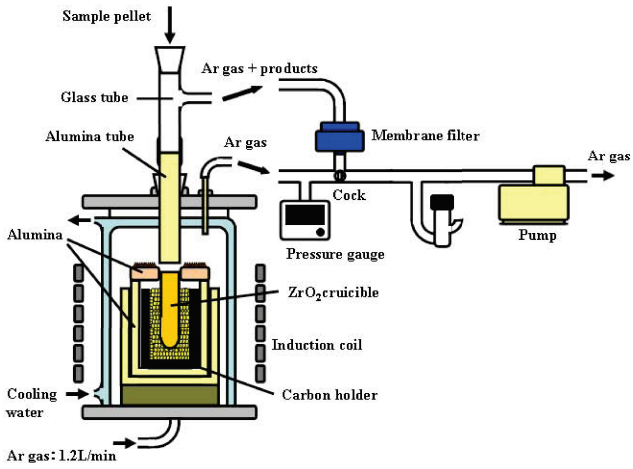


**Figure 1.** Schematic experimental set-up for high temperature reduction of silica.

### 2.2 Reduction Reaction

High temperature reduction was carried out in a zirconia crucible (o.d. = 25 mm, i.d. = 20 mm, height = 100 mm) which was heated by induction furnace via a carbon holder. Figure 1 shows the schematic experimental set-up. The crucible, carbon holder, and the alumina holders were put in a double-walled quartz reactor, which was cooled with water. The reaction was carried out in argon atmosphere. Argon carrier gas with the flow rate of 1.2 L/min was introduced from the bottom of the reactor. After the temperature of the crucible, measured by a pyrometer, was stabilized at 2073 K, sample pellets were quickly introduced from the upper glass tube, which was connected with an alumina tube (o.d. = 25 mm, length = 300 mm), to a zirconia crucible. The pressure inside the reactor was slightly reduced with help of a diaphragm pump so that the reaction products flow upward towards a membrane filter (Pore size 0.10 μm, Advantec).

### 2.3 Characterization of Products

After the reaction, products distribute at membrane filter, glass tube, and alumina tube, and inside the crucible. The last type of products is not considered in the present paper because our main concern is the deposition product. In our previous studies on carbothermal reduction of silica-containing slag, it was shown that the morphology of reaction products changes at different deposition temperature. Therefore, we collected the products separately, namely at filter, glass tube, upper half and lower half of alumina tube. The products were characterized by XRD (XRD-6100, Shimadzu), SEM (JSM-6060, JOEL), and TEM (H-800, Hitachi).

### 2.4 HF Treatment of Reduction Products

The silicon dioxide, formed in disproportionation reaction, was removed by adding 100 mg of reduction products into 50 mL of aqueous HF solution (46–48 mass%, Wako pure chem.) for 30 min. It should be here noted that the HF solution was bubbled with argon gas for 30 min prior to the addition of reduction products and during the dissolution treatment in order to remove the dissolved oxygen in the solution. The solution was then filtered with a membrane filter (Pore size 0.10 μm, Advantec). The powders remaining on the filter were characterized by the analytical equipments mentioned above.

## 3 Results and Discussion

### 3.1 Products Identification

Figure 2 shows the XRD patterns of reaction products collected at different positions. A broad peak around $2\theta \sim 25°$ can be attributed to amorphous SiO and/or $SiO_2$. It is clearly seen that the diffraction peaks of silicon are found in all reaction products but the reaction products collected at alumina tube contain crystalline silica as well as quartz. The latter is presumably the initial quartz in the sample, which may be due to the splash phenomena, i.e., transfer by carrier gas, at the initial stage of the reaction. In comparison

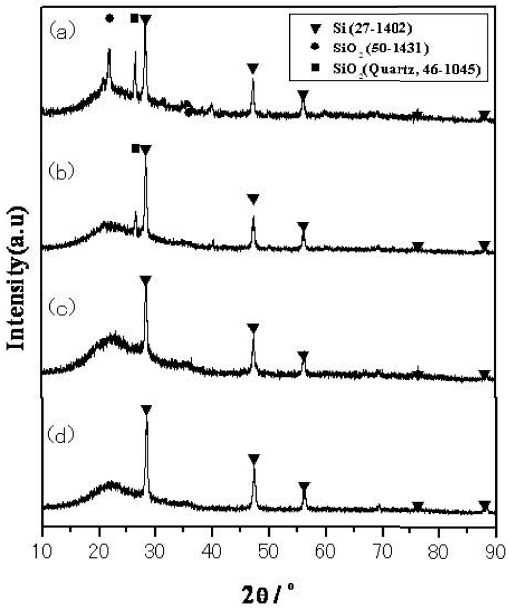


**Figure 2.** XRD patterns of reaction products collected at (a) lower part of alumina tube (i.e., from bottom to 15 mm above bottom of the tube), (b) upper part of alumina tube (from 15 mm above bottom to the top of tube, i.e., 30 mm above bottom), (c) glass tube, (d) filter. The composition is $[SiO_2] : [Ti] = 1 : 0.7$ in molar ratio. The powder diffraction file number is listed in the legend.

| $[SiO_2]$ : [Ti] | 1 : 0.5 | 1 : 0.7 | 1 : 1 | 1 : 2 |
|---|---|---|---|---|
| Gram of product/1 g of initial $SiO_2$ | 0.027 | 0.043 | 0.041 | 0.024 |

**Table 1.** Product yield collected at filter.

to the carbothermic reduction of silica, the reduction by titanium leads to the significant suppression of the formation of silicon carbide. It should be noted that the intensity of X-ray diffraction peaks of $\beta$-SiC is comparable to that of Si in carbothermic reduction [6].

The diffraction peaks of silicon in the sample collected at filter are stronger than those collected at positions closer to the reactor. This indicates that the concentration of metallic silicon in the products at filter is higher than those collected at different positions. Taking this result and the results of our previous study on the carbothermic reduction of silica-containing slag into account, we focus on the products captured at filter.

### 3.2 Influence of the Composition on the Reaction Products at Filter

The variation of the composition changes the activity of the relevant species, so that the products distribution and the phases can change. Figure 3 shows the XRD pattern of products at filter with different initial sample compositions. Sharp diffraction peaks of silicon are observed in all the cases. However, their relative intensity against the broad background peak around $2\theta \sim 25°$ varies with composition, i.e., they are highest at $[SiO_2]$ : [Ti] = 1 : 0.7. It is

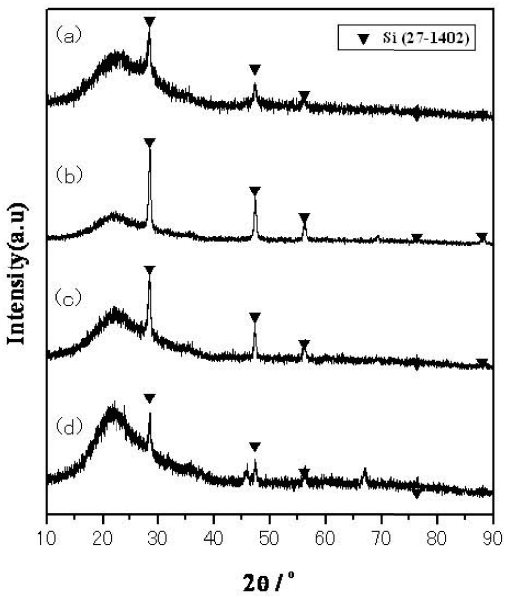


**Figure 3.** XRD patterns of reaction products collected at filter for the composition of $[SiO_2]$ : [Ti] = (a) 1 : 0.5, (b) 1 : 0.7, (c) 1 : 1 and (d) 1 : 2 in molar ratio.

expected that the composition of $[SiO_2]$ : [Ti] = 1 : 0.5 is stoichiometrically required for the SiO formation, i.e., $SiO_2 + (1/2)Ti = SiO + (1/2)TiO_2$. The present result shows that slightly higher amount of titanium is optimum with respect to the concentration of silicon in the products. The increase in the titanium composition from $[SiO_2]$ : [Ti] = 1 : 1 to 1 : 2 leads to the decrease in the relative intensity of diffraction peaks of silicon. It is known that silicon and titanium form various intermetallic compounds [7]. Thus, the decrease in activity of silicon in melts may be responsible for the decrease in the amount of silicon in reaction products. We should also remark the yield of products collected at filter, which is summarized in Table 1. The yield is, in general, low, i.e., a few percents of the initial $SiO_2$. This is expected because the equilibrium reaction is presumably the reduction of silica to metallic silicon, represented by $SiO_2 + Ti = Si + TiO_2$. In the case of $[SiO_2]$ : [Ti] = 1 : 2, the product yield is very low, which indicates the low activity of silicon.

As for the size of the silicon crystallites, Scherrer's equation for the X-ray diffraction peaks of silicon was employed [8]. We obtained the size of $\sim$20 nm. The composition dependence on the size was not observed.

The SEM images of the products at filter are shown in Figure 4. The products consist of fibrous and particulate materials with the size of 10–100 nm. A SEM-EDS (energy dispersion spectra) analysis showed that the most intense X-ray fluorescence of silicon was observed at the composition of $[SiO_2]$ : [Ti] = 1 : 0.7 in accordance with the results of XRD. There is a tendency where the concentration of silicon correlates with the relative amount of fibrous products.

### 3.3 TEM Analysis

TEM images of both fibrous and particulate products are shown in Figure 5 and Figure 6, respectively. As seen in Figure 5, dark parts indicate the existence of crystalline materials. They are crystalline silicon, as shown in diffraction pattern where diffraction spots, corresponding to that of (111) plane of silicon, is observed. On the other hand, particulate materials are mainly amorphous, as depicted in their diffraction patterns (Figure 6). The energy dispersive spectra indicate that the relative amount of oxygen in particulates is higher than that in fibres, the former is presumably amorphous SiO and/or $SiO_2$, and the metallic silicon is enriched in amorphous fibre matrix.

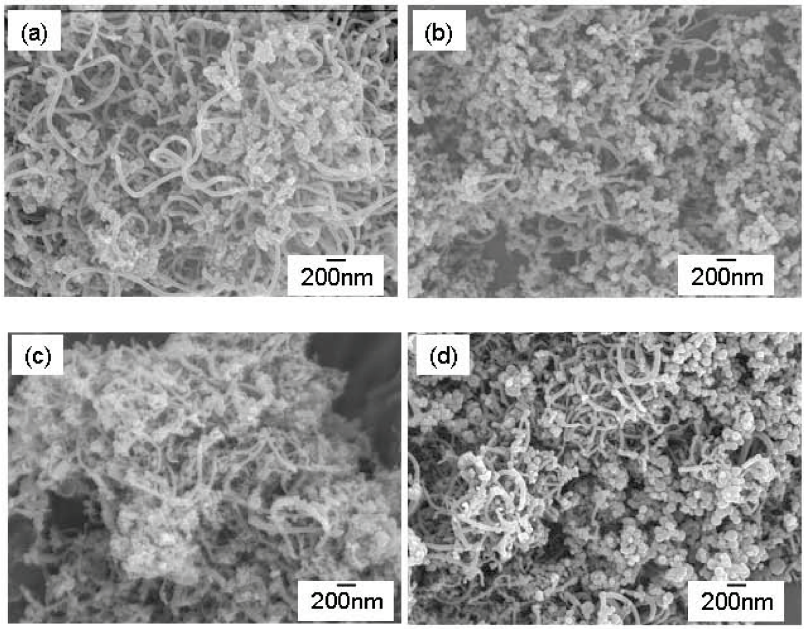


**Figure 4.** SEM images of the reaction products collected at filter for the composition of $[SiO_2]$ : $[Ti] =$ (a) 1 : 0.5, (b) 1 : 0.7, (c) 1 : 1 and (d) 1 : 2 in molar ratio.

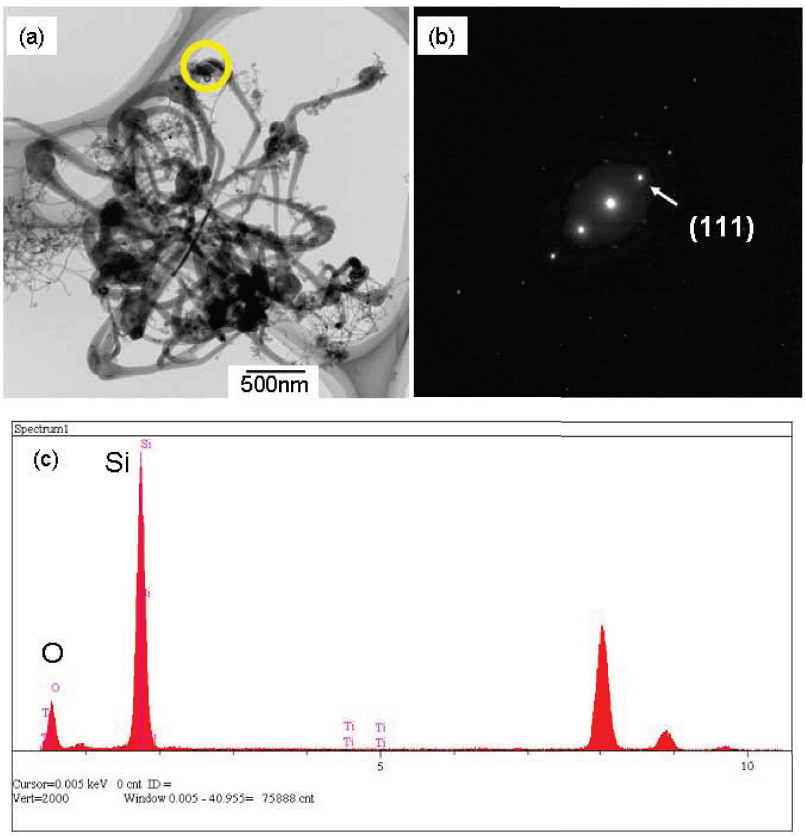


**Figure 5.** (a) TEM image of the fibrous products collected at filter. (b) Electron diffraction pattern from the circle region in the TEM image. (c) Energy dispersive spectra obtained from the whole region of the TEM image. The peak intensity is normalized by that of silicon at $\sim 1.7$ keV. The composition is $[SiO_2] : [Ti] = 1 : 0.7$ in molar ratio.

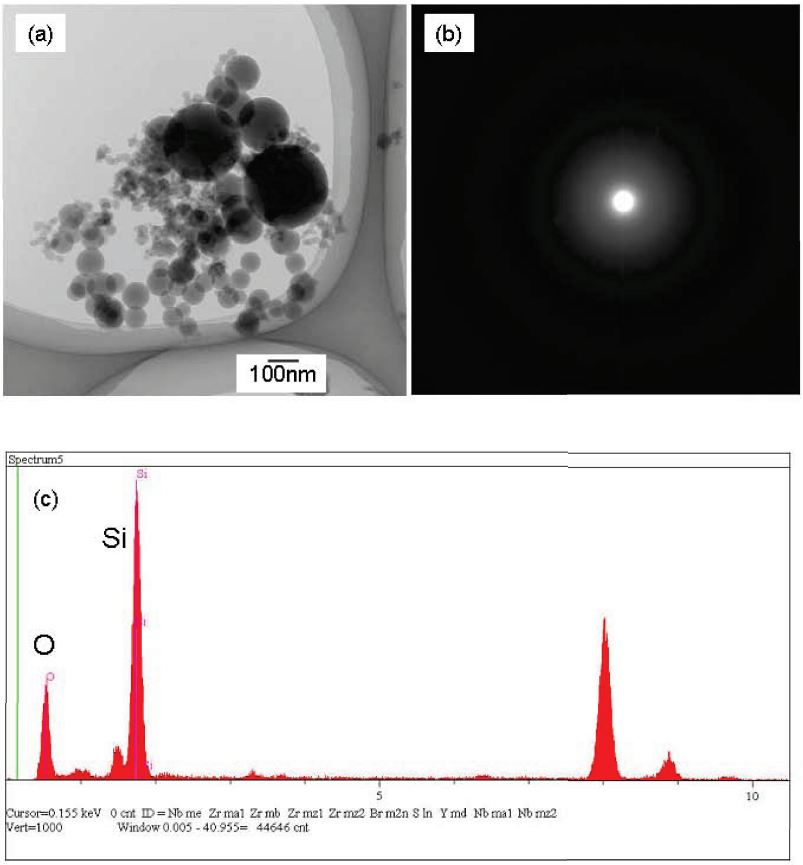


**Figure 6.** (a) TEM image of the particulate products collected at filter. (b) Electron diffraction pattern obtained from the whole region of the TEM image. (c) Energy dispersive spectra obtained from the whole region of the TEM image. The peak intensity is normalized by that of silicon at $\sim 1.7$ keV. The composition is $[SiO_2] : [Ti] = 1 : 0.7$ in molar ratio.

### 3.4 Attempt to Remove Silicon Dioxide in Reaction Products

As mentioned above, reaction products contain amorphous particulates and crystalline silicon particles in amorphous wires. As far as the disproportionation reaction of SiO is employed, the formation of $SiO_2$ cannot be avoided. In order to establish a process of the silicon particles production, it is essential to enrich the crystalline particles. Therefore, we have carried out the hydrofluoric treatment of reaction products. Figure 7 shows the SEM images of the starting and HF-treated materials. Obviously, the relative amount of the particles is increased by the acid treatment, indicating the removal of amorphous fibrous materials. Figure 8 shows the TEM image of a HF-treated material and the corresponding electron diffraction pattern. The materials are silicon with the size of $\sim 10$ nm.

The present method is very promising for the production of silicon particles. However, there are several difficulties, such as low yield of silicon particles and very sensitive property against oxidation. A precise control of particle size distribution is also desired. Further optimization of

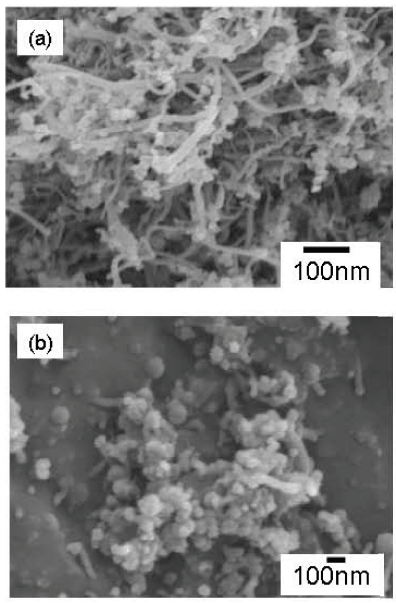


**Figure 7.** SEM image of a reaction product collected at filter (a) before and (b) after HF treatment.

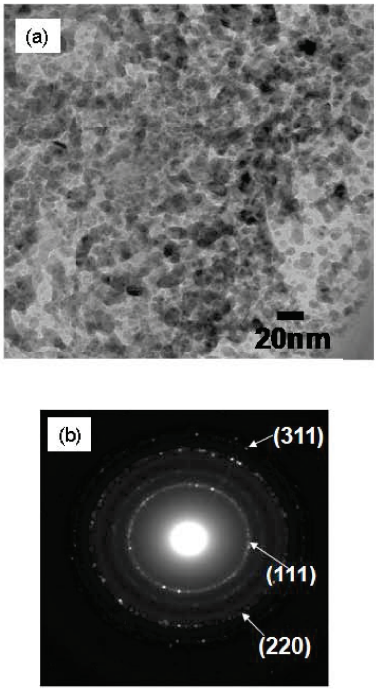


**Figure 8.** (a) TEM image of the reaction product collected at filter after HF treatment, (b) its electron diffraction pattern.

the process parameters, such as a precise control of reaction atmosphere and carrier gas flow rate and the utilization of protective coating of the particles, is needed.

## 4 Conclusion

In the present study we addressed the formation of nanoscale Si-based materials which were produced by the reduction of silica by titanium at 2073 K. The reaction products precipitates were silicon-based fibrous and particulate materials with the order of 10–100 nm. In comparison to results of carbothermic reaction, the contamination of silicon carbide was significantly suppressed. Further treatment of products can enrich the silicon particles. At present the final yield of the particles is less than 1% of the initial $SiO_2$ after HF treatment, so that further optimization of the process parameters is needed.

## Acknowledgments

We acknowledge Dr. Shigeo Arai (Eco Topia Science Institute, Nagoya Univ.) for his kind support in TEM measurements.

## References

[1] H. Kamimura, Y. Kanemitsu, M. Kondo and K. Takeda ed., "Light emission from novel silicon materials", *J. Phys. Soc. Jpn. Supplement B*, **63** (1994).

[2] M. Mamiya, H. Takei, M. Kikuchi and C. Uyeda, "Preparation of fine silicon particles from amorphous silicon monoxide by the disproportionation reaction", *J. Cryst. Growth*, **229** (2001), 457.

[3] V. Kapaklis, "Structural characterization of silicon nanocrystals from amorphous silicon oxide materials", *J. Non-cryst. Solids*, **354** (2008), 612.

[4] W. Dewald, C. Borschel, D. Stichtenoth, T. Niermann and C. Ronning, "Phase diagram of Si nanowire growth by disproportionation of SiO", *J. Cryst. Growth*, **312** (2010), 1751.

[5] S. V. Komarov, D. V. Kuznetsov, V. V. Levina and M. Hirasawa, "Formation of SiO and related Si-based materials through carbothermic reduction of silica-containing slag", *Mater. Trans.*, **46** (2005), 827.

[6] S. V. Komarov, D. V. Kuznetsov, O. Terakado, V. V. Levina and M. Hirasawa, "Characterization of Si-based nanoparticulates produced by carbothermic reduction of silica-containing slag", *Mater. Trans.*, **46** (2005), 3044.

[7] H. Okamoto, *Desk Handbook Phase Diagrams for Binary Alloys*, ASM International, OH, (2000).

[8] B. D. Cullity, *Elements of X-ray Diffraction*, Addison-Wesley, (1956).